

Facile Synthesis of Activated Carbon/Alginate/Chitosan Composite Beads as Rhemazole Brilliant Blue R Adsorbent

Dhony Hermanto^{1*}, Putri Jauhar Prihatini¹, Niza Yusnita Apriani¹, Lely Kurniawati¹, Murniati Murniati¹, Sapriani Hamdiani¹, Nurul Ismillayli¹, Siti Raudhatul Kamali²

¹ Department of Chemistry, Faculty of Mathematics and Natural Science, University of Mataram, Indonesia

² Department of Environmental Science, Faculty of Mathematics and Natural Science, University of Mataram, Indonesia

Corresponding Authors E-mail: dhony.hermanto@unram.ac.id

Article Info	Abstract
<p>Article info: Received: 10-06-2024 Revised: 14-08-2024 Accepted: 18-08-2024</p> <p>Keywords: Activated carbon/ alginate/ chitosan; Composite Beads; Rhemazole Brilliant Blue R</p> <p>How To Cite: D. Hermanto, P. J. Prihatini, N. Y. Apriani, L. Kurniawati, M. Murniati, S. Hamdiani, N. Ismillayli, and S. R. Kamali, "Facile Synthesis of Activated Carbon/ Alginate/ Chitosan Composite Beads as Rhemazole Brilliant Blue R Adsorbent," <i>Indonesian Physical Review</i>, vol. 7, no. 3, p 480-495, 2024.</p> <p>DOI: https://doi.org/10.29303/ipr.v7i3.343</p>	<p>Developing composite beads composed of chitosan, alginate, and activated carbon for dye removal is essential due to their improved adsorption capabilities and environmental benefits. By utilizing natural resources efficiently for an effective dye removal process, this study developed an activated carbon/alginate/chitosan composite bead as Rhemazole Brilliant Blue R (RBBR) adsorbent. The surface shape of composites exhibits more protrusions, grooves, and asymmetric pores than activated carbon, which could improve dye adsorption capability. FTIR analysis verified that functional groups such as OH, NH, protonated amine, and carboxylate from the constituent polymers were enriched in the activated carbon/alginate/chitosan composite. These groups also function as active sites for adsorbents. It was aligned with the composite beads' Freundlich isotherm model, which shows that heterogeneous or many active sites contribute to adsorption and provide multilayer adsorption. The kinetic model of pseudo-second order fits well with the adsorption process, indicating that chemisorption is the rate-limiting step in RBBR adsorption. The optimum adsorption conditions were at pH 1, with an adsorbent dose of 0.08 g, RBBR dye concentration of 125 mg/L, and a contact time of 60 min. The composite beads also exhibit stability in acidic and basic solutions, with the effectiveness of being reused up to four times, providing a reusable adsorbent with versatility in various water treatment conditions. Hence, synthesizing activated carbon/alginate/chitosan composite beads presents a promising solution for sustainable wastewater treatment based on biodegradable and eco-friendly composite.</p> <p>Copyright © 2024 Authors. All rights reserved.</p>

Introduction

More than 735 tons of dyes are produced by the textile industry each year, comprising 40,000 different dyes with over 7000 distinct chemical structures [1]. During the industrial processes, many dyes of waste are released by nature, leading to water disposal problems. Textile dyes have been classified according to their chemical structure, e.g., azo, nitro, indigo,

anthraquinone, phthalein, triphenyl methyl, nitrated, etc. Among them, pollution with anthraquinone dye, especially Remazol Brilliant Blue R (RBBR) [2,3], has recently attracted more attention owing to the severity of the pollution caused by RBBR in the environment. RBBR dye has good chemical stability and makes it difficult to degrade by the conventional process. Due to its very hazardous properties, this dye waste can cause allergies, skin irritation, genetic alterations, and cancer. It will also disturb the aquatic habitat [4]. Removal of RBBR is important to creating a sustainable society.

Many methods exist to remove dyes in water such as ion exchange, coagulation, phyto-degradation, reverse osmosis, electro-dialysis, and microbiology [5-7]. Still, most of these methods are quite expensive, require certain materials, and require high technology to be applied. Another widely used water-treating technique is adsorption. Effective and efficient processes, high absorption capacities, ability to reusability, low operational costs, and lack of negative side effects of adsorbent are potential benefits of adsorption techniques [8]. Adsorption techniques can stop dye pollution from spreading throughout the environment, especially in water.

Activated carbon is the most widely used adsorbent because it has a larger surface area than other adsorbents, it can absorb more adsorbate molecules. This is due to the dye-absorbing pores in activated carbon [9-11]. One frequent active carbon source that can be used as a dye adsorbent is water hyacinth waste [12]. The poor absorption of polar components is the drawback of activated carbon adsorbents [13]. The alteration properties of the surface functional group on the activated carbon indicated that appropriate treatments could enhance its functionality. The excellent properties of bio-composite materials make it an ideal material to combine with activated carbon and can further improve adsorbent performance. Abundant functional groups are mainly associated with heteroatoms present on the bio-composite surface and often modified to increase their adsorption capability. Modified activated carbon using chitosan and pectin synthesized into bead composite has been used for adsorbed methylene blue dye [14]. Other modified activated carbon using chitosan and alginate synthesized into bead composite has been used for adsorbed methylene blue and methyl violet 2B dye with maximum adsorption capacities of 1.34 mmol/g for MB and 1.23 mmol/g for MV 2B [15]. Modification of activated carbon with composite-based polyelectrolyte complex (PEC) has the potential to increase the availability of pores and reactive functional groups in the adsorbent surface, it promises to increase adsorbent capabilities.

This study developed composite beads by combining alginate-chitosan PEC with activated carbon and CaCl_2 as a crosslinker. Alginate is polyanionic, whereas chitosan is polycationic. Once polyelectrolyte complexes (PEC) develop, the amino groups of chitosan and the carboxyl groups of alginate are involved in self-electrostatic interactions that allow these polymers to connect [16,17]. Adding CaCl_2 as a cross-linking agent increases the structural integrity, and regular pores are formed, resulting in an orchestrated network structure inside the hydrogel beads. Divalent cations (Ca^{2+}) can increase the adsorption capacity of negatively charged adsorbates (anions anthraquinone) [14,15]. Thus, this research's main objective is to investigate the possibility of composite beads consisting of activated carbon, alginate, chitosan, and CaCl_2 (crosslinker) as RBBR color adsorbers. The pH, amount of adsorbent, and dye concentration were optimized for optimal adsorption. Furthermore, the kinetic study, adsorption isotherm model, and adsorption capacity are described.

Experimental Method

Chemicals

Water hyacinth collected from the Aik Bukak Lombok dam provided the activated carbon employed in the investigation. Water hyacinth is a perennial aquatic plant that floats freely in waters, can quickly increase biomass, forms dense mats, and reproduces from stolons; its dominant chemical composition is cellulose and hemicellulose [12]. Additional research chemicals used in this work were RBBR (from Dystar), chitosan (from Sigma Life Science), and sodium alginate (from Sigma-Aldrich). The analytical grade from Merck was attained for acetic acid (CH_3COOH), hydrochloric acid (HCl), nitric acid (HNO_3), sodium hydroxide (NaOH), and calcium chloride (CaCl_2). Double distilled water was used in all solution preparation and dilution.

Preparation of Activated Carbon

After cleaning, the water hyacinth samples were dried. The samples were mixed after being dried for 24 h at 110 °C in the oven. Afterward, the dried samples were carbonized at 600 °C in a furnace for 1 h and N_2 atmosphere. The carbon has activated after being soaked for 24 h in 0.1 M HCl. After the samples were filtered, 0.1 M NaOH was used to neutralize the activated carbon, and distilled water was used to rinse it, then dried for 1 h at 110 °C in the oven [18]. The activated carbon was stored in a desiccator until used.

Formation of Activated Carbon/Alginate/Chitosan Composite Beads

The synthesizing composite beads were executed by modifying the study methodology employed by Rahmah et al. [14] and Hermanto et al. [19]. To create chitosan hydrosol, 1 g of chitosan was dissolved in 10 mL of double distilled water, and 5 mL of 2% acetic acid was added. The mixture was agitated for 4 hours and left overnight. Then, CaCl_2 was added to the mixture solution and stirred again until homogeneous to form chitosan hydrosol. To create alginate hydrosol, 1 g of alginate was dissolved in 14 mL of double distilled water in a separate container, mixed until homogenous, and left overnight. Next day, stir the alginate hydrosol after adding 1 g of activated carbon. Composite beads were created by injecting 5 mL of alginate hydrosol into the chitosan hydrosol while stirring. Following formation, the composite beads were cleaned, dried in the oven at 60 °C, and filtered. FTIR was used to characterize composite beads. The composite beads were stored in a desiccator until used.

Effect of pH on Dye Adsorption

A range of pH 1-9 dye solutions were made, each containing 20 mg/L RBBR in buffer solution. Add 0.001 g of composite bead powder to an Erlenmeyer flask and 10 mL of the series dye solution immediately. At room temperature, shaking was done for 30 min at 200 rpm. After filtering the solid material, the UV-Vis spectrophotometer examined the filtrate dye solution at 630 nm.

Effect of Adsorbent Dose on Dye Adsorption

Activated carbon/alginate/chitosan composite beads in dosages of 0.02, 0.04, 0.06, 0.08, and 0.1 mg were used to study the impact of adsorbent dose. The 500 mgL^{-1} RBBR dye solution contained 10 mL of the various adsorbent dosages added to it. The ideal pH was achieved by adjusting the solution to that found in the earlier experiment. After that, the adsorption process lasted for 30 min at shaking conditions with speed of 80 rpm. Following the separation of the solid material, spectrophotometry UV-Vis was used to examine the dyes at 630 nm that had been filtered.

Effect of Dye Concentration on Dye Adsorption

Various dye concentrations (50, 75, 100, and 125 mg/L) were tested to see what effect they had. As determined by the results of the previous experiment, 0.001 g of composite bead was introduced to the dye series solution. At room temperature, shaking was done for 30 minutes at 200 rpm. Following the separation of the solid material, spectrophotometry UV-Vis was used to examine the dyes at 630 nm that had been filtered.

Effect of Contact Time on Dye Adsorption

A time range of 5 to 180 minutes was used to determine the impact of contact time. Activated carbon/alginat/chitosan composite beads from the previous experiment at their optimal adsorbent dose were added to 10 mL of 50 ppm RBBR dye solution at pH 1. After that, the adsorption process lasted for 45, 60, 75, and 90 min at shaking conditions of 80 rpm. Following the separation of the solid material, spectrophotometry UV-Vis was used to examine the dyes at 630 nm that had been filtered.

Kinetic Study of Adsorption

The RBBR adsorption kinetics were investigated using pseudo-first-order, pseudo-second-order, and intraparticle diffusion adsorption models. The RBBR dye adsorption process was carried out with 30, 45, 60, 75, and 90 min contact times. Equation (1) was used to quantify the quantity of RBBR dye adsorbed (q_t , mg g⁻¹), while equations (2), (3), and (4) showed the pseudo-first order, pseudo-second order, and intraparticle diffusion reaction equations) [20], respectively.

$$q_t = \frac{(C_0 - C_t)V}{W} \tag{1}$$

$$\ln(q_e - q_t) = \ln q_e - k_1 t \tag{2}$$

$$\frac{t}{q_t} = \frac{t}{q_e} + \frac{1}{k_2 q_e^2} \tag{3}$$

$$q_t = (k_{int} t^{1/2}) + C \tag{4}$$

Where C_0 and C_t are the initial and time t concentrations of RBBR dye (mg L⁻¹), V is the volume of solution (L), W is the mass of the composite adsorbent, and q_e is the amount of RBBR adsorbed on the composite at equilibrium (mg g⁻¹). While k_1 , k_2 , and k_{int} are the pseudo-first-order reaction rate, pseudo-second-order reaction rate, and intraparticle diffusion constant, respectively, C (mg g⁻¹) is a constant proportional to the thickness of the boundary layer.

Isotherm Model for Dye Adsorption

The isotherm adsorption model determines RBBR based on the variation in concentration at the ideal pH and adsorption data. Both the Freundlich and Langmuir adsorption isotherms were employed in this investigation. The reversible nature of adsorption in a monolayer is the basis of the Langmuir equation, expressed in Eqs. 5 and 6. Utilizing Eqs. 7 and 8, the Freundlich isotherm formula was obtained [21].

$$Q_e = \frac{Q_m \times K_L \times C_e}{(1 + K_L C_e)} \tag{5}$$

$$\frac{C_e}{Q_e} = \frac{1}{Q_m K_L} + \frac{C_e}{Q_m} \tag{6}$$

$$Q_e = \frac{x}{m} = K_f + C_e^{1/n} \quad (7)$$

$$\log Q_e = \log K_f + \frac{1}{n} \log C_e \quad (8)$$

Where: m is the mass of adsorbent (g); V is the volume of solution (L); Q is the adsorption capacity per molecular weight (mg/g); maximum adsorption capacity (Q_m) is expressed in mg/g, while adsorbed adsorbate at equilibrium (Q_e) is expressed in mg/g; C_0 is the initial concentration of the solution (ppm); C_e is the final concentration of the solution (ppm); K_f and n are Freundlich constants, K_L is the Langmuir constant.

Reusability Test

The composite reuse test is closely related to the composite life cycle, and it suggests utilizing composites as adsorbents that are still effective. The test involved five adsorption and desorption cycles using the same composite adsorbent. The adsorption procedure was carried out under optimal conditions, which included a composite mass of 0.08 g, an RBBR dye concentration of 125 mg/L, pH 1, and a contact period of 60 min. Centrifugation at 5000 rpm for 30 minutes separated the composite that absorbed the RBBR dye. The composite's desorption was carried out by adding 10 mL of dilute NaOH solution (1 mM) at room temperature for 10 minutes while stirring. Spectrophotometry UV-Vis determined the concentration of RBBR dye at 630 nm. %Reuse efficiency in each cycle was determined by equation 9, where n is the 2nd, 3rd, 4th, and 5th cycles.

$$\% \text{ Reuse Efficiency} = \frac{\% \text{adsorption}_n}{\% \text{adsorption}_1} \times 100\% \quad (9)$$

Result and Discussion

Morphological Study

The composite was made by mixing alginate hydrosol with activated carbon, then adding dropwise by stirring into the chitosan hydrosol mixed with the CaCl_2 crosslinking agent. The composite formed was a round, solid, hard, black granular material with uniform size and shape. The results of synthesizing activated carbon/alginate/chitosan composite beads can be seen in Figure 1.

Figure 1(a) shows an image of the synthesized activated carbon/alginate/chitosan composite beads. The black-colored granule beads show that the activated carbon has been immobilized into the composite material. Figure 1(b) is an SEM image of the surface morphology of activated carbon from water hyacinth. Porous carbon particles can be seen on the activated carbon surface [22]. An SEM image of the surface morphology of the PEC alginate-chitosan composite is shown in Figure 1(c).

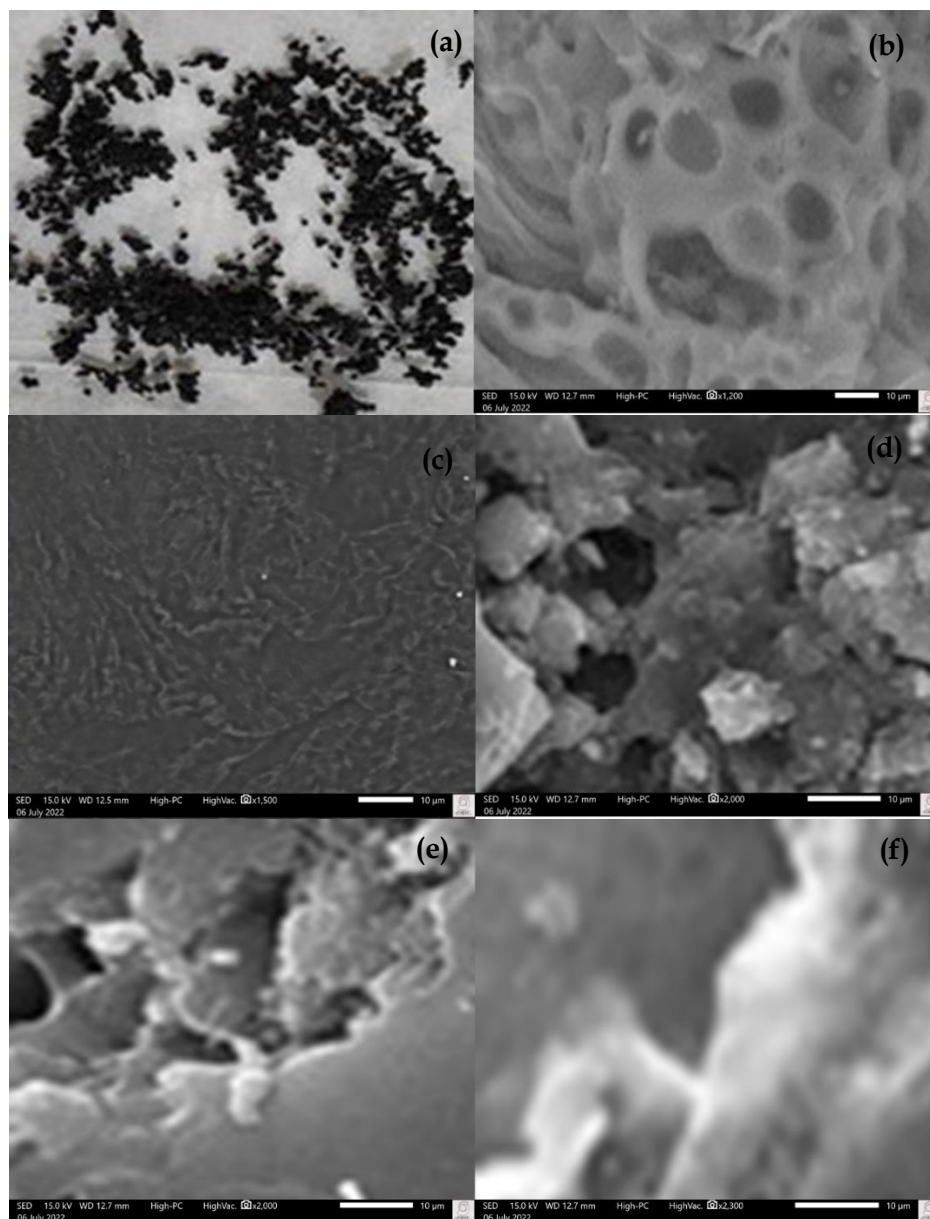


Figure 1. (a) Photograph of activated carbon/alginate/chitosan beads composite, SEM images for (b) activated carbon, (c) alginate-chitosan PEC composite, (d) activated carbon/alginate/chitosan beads composite, (e) after adsorption of RBBR, and (f) after desorption of RBBR, respectively.

Previous studies have demonstrated that a fibrous matrix with an uneven form and rough appearance appears to be an interconnected structure of electrostatic interactions between chitosan and alginate [23]. Figure 1(d) is an SEM image of the surface morphology of the synthesized activated carbon/alginate/chitosan composite beads. The surface morphology shows protrusions, grooves, and asymmetric pores. This is because the upper part of the composite is suspended while the lower part undergoes a mobilization process. The activated carbon is evenly distributed in the composite. The synthesized activated carbon/alginate/chitosan composite beads appear to have larger pores than activated carbon. Chemical modification of activated carbon with alginate-chitosan via PEC composite can expand the pore size of carbon, it has the potential to increase the dye absorption capacity.

Based on Figure 1(e), the adsorption of RBBR dye causes the surface of the activated carbon/alginate/chitosan composite bead to become rough, with lumps covering the pores of the activated carbon. These lumps represent how the adsorbate (RBBR dye) and the adsorbent (composite bead) interact, leading to adsorbate trapped in the pores of the composite bead. The SEM image of the activated carbon/alginate/chitosan composite bead after desorption with ethanol shows a lumpy surface with closed pores. This indicates that the desorption process is followed by the activated carbon/alginate/chitosan composite bead's surface releasing an adsorbent substance.

FTIR Analysis

The activated carbon/alginate/chitosan composite beads' distinctive functional groups were identified via FTIR analysis, as seen in Figure 2.

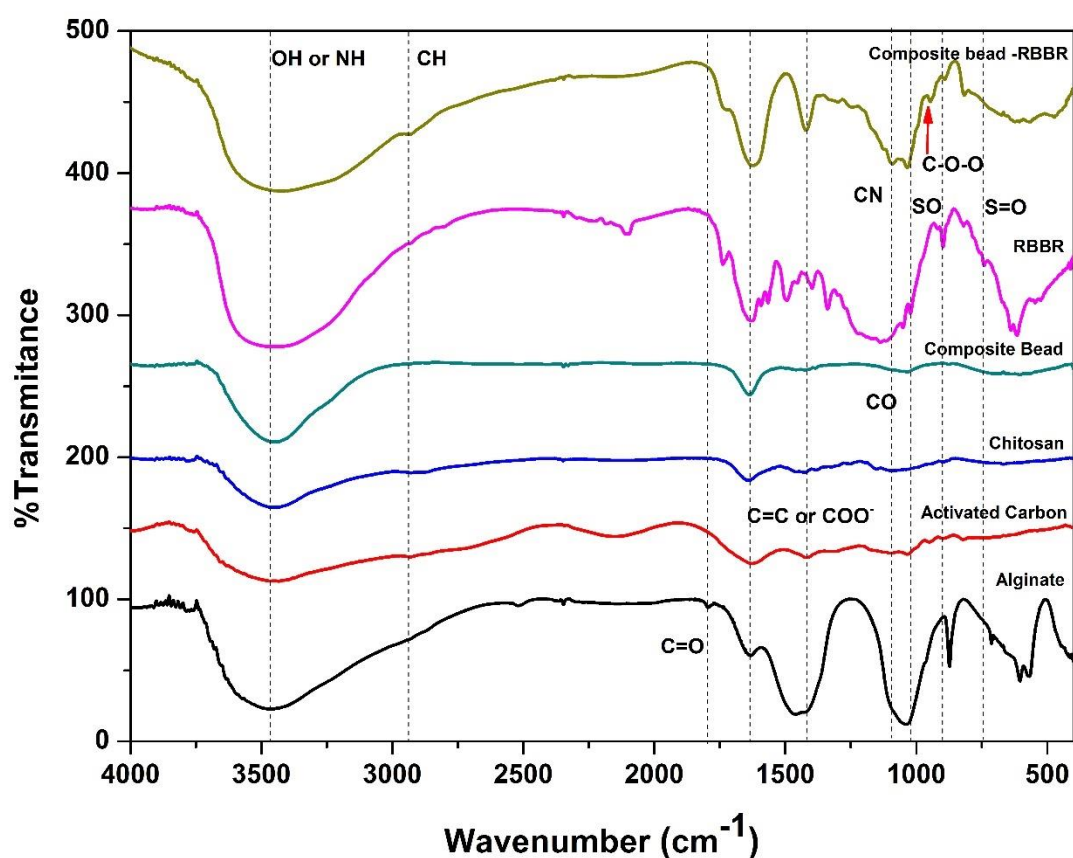


Figure 2. FTIR spectra of (a) activated carbon, (b) alginate, (c) chitosan, (d) activated carbon/alginate/chitosan composite bead, (e) RBBR dye, and (f) activated carbon/alginate/chitosan composite bead with RBBR dye, respectively.

According to Figure 2, the FTIR spectra reveal the functional groups owned by the composite and its components. As a precursor material, activated carbon contains an OH functional group, as evidenced by an absorption band at 3467 cm^{-1} . The existence of C=O, C=C, and C-O groups is indicated by absorption at 1795 , 1632 , and 1039 cm^{-1} . The absorption of 1459 cm^{-1} suggests the bending of the C-H group, which is supported by the absorption of 873 cm^{-1} . In

contrast, the C-C stretching is indicated by absorptions of 712 and 604 cm^{-1} [24,25]. The characteristic peaks of chitosan have been observed at 3465, 1639, 1543, and 1324 cm^{-1} , which correspond to the OH or N-H group vibrations, C=O (from amide I), the N-H group bending (from the primary amine), and C-N stretching. Absorption at 2930 and 2880 cm^{-1} reveals both symmetric and asymmetric C-H vibrations. While absorption at 1425 and 1387 cm^{-1} indicates the bending of CH_2 and CH_3 , absorption at 1089 cm^{-1} is attributed to C-N (primary amine) stretching [26,27]. Alginate spectra show absorption at 3434, 2931, 2870, 1625, and 1418 cm^{-1} due to OH group vibrations, symmetric and asymmetric C-H, and symmetric and asymmetric stretching COO^- (from carboxylate). Absorption at 1097, 1033, and 950 cm^{-1} indicates C-O stretching (from pyranosyl ring and uronic acid residue) [28,29]. The composite spectra indicate the combined absorption of the precursor substances, with some absorptions shifting and disappearing. The absorption of the OH group shifts slightly to 3464, indicating the presence of hydrogen bonding interactions in the composite. The absorption of the primary amine functional group in chitosan (1543 cm^{-1}) and C-N stretching of primary amine (1089 cm^{-1}) were not identified in the composite, indicating that $-\text{NH}_2$ was protonated ($-\text{NH}_3^+$) due to the addition of acetic acid to chitosan during the composite's synthesis [19,24,30]. The shift in the absorption of alginate's carboxylate functional groups from 1625 and 1418 to 1638 and 1463 cm^{-1} suggests that these groups interact with other groups, possibly NH_3^+ . FTIR examination revealed the enrichment of functional groups in activated carbon/alginate/chitosan composite, including hydroxyl, protonated amine, carbonyl, and carboxylate from the constituent polymers.

RBBR dye shows the absorption peak at 3435, 1738, 1629, 1591, and 1050 cm^{-1} , indicating the presence of NH/OH, C=O, C=C, N-H, and C-O groups. The characteristic groups of S=O and C-CO-C of RBBR dye were indicated by absorption at 740 and 638-615 cm^{-1} [31]. Interaction of RBBR dye and the activated carbon/alginate/chitosan composite possibly occurred at many active composite sites, indicated by peak shifting of the composite before and after adsorption, as shown in Figure 2. The shift occurs in the absorption of the -OH or N-H group, which widens from 3465 to 3414 cm^{-1} , as well as the absorption of carboxylate groups (COO^-) at 1638 and 1463 to 1623 and 1421 cm^{-1} [32]. Since SO_3^{2-} is the active group of RBBR dye, its functional groups can interact with carboxylate groups through the NH_3^+ group and Ca^{2+} bridges. In contrast, the interaction between RBBR functional groups and OH or N-H groups of the composite can occur through hydrogen bonds with a broad peak characteristic. It is supported by the disappearance of S=O absorption by RBBR dye at 740 cm^{-1} . Previous research has demonstrated the role protonated amine groups play in dye adsorption [33,34]. Adsorption of RBBR dye on the composite surface is evidenced by the appearance of RBBR peaks on the composite following adsorption, such as 1726 cm^{-1} (C=O), 1391 cm^{-1} (CH_3), and 892 cm^{-1} (C-H). Furthermore, the appearance of a new peak in the composite bead-RBBR spectra around 948 cm^{-1} (C-O-O) [26] as indicated by the red arrow in Figure 2, suggests the formation of a new bond composite with RBBR during the adsorption process. This allows for the presence of various mechanisms in adsorption, including chemisorption. The FTIR study verified that the -OH, N-H, carboxylate, and protonated amine functional groups of the composite serve as the adsorbent's active sites.

The pH, Composite Bead, RBBR Concentration, and Contact Time Effect

Choosing pH is a crucial factor in establishing the ideal adsorption state. The pH range of 1-9 was utilized to explore the effect of pH on activated carbon/alginate/chitosan composite beads' RBBR dye adsorption. The adsorbent dosage is one of the factors affecting the RBBR dye adsorption process. It was examined at dosages of 0.02, 0.04, 0.06, 0.08, and 0.1 mg of the activated carbon/alginate/chitosan composite beads. Furthermore, contact time is a significant aspect of the adsorption process, as it refers to the time required to stir between the composite beads and the dye solution. Figure 3 depicts the dependence curve of the adsorption efficiency versus pH, bead composite dosage, RBBR dye concentration, and contact duration.

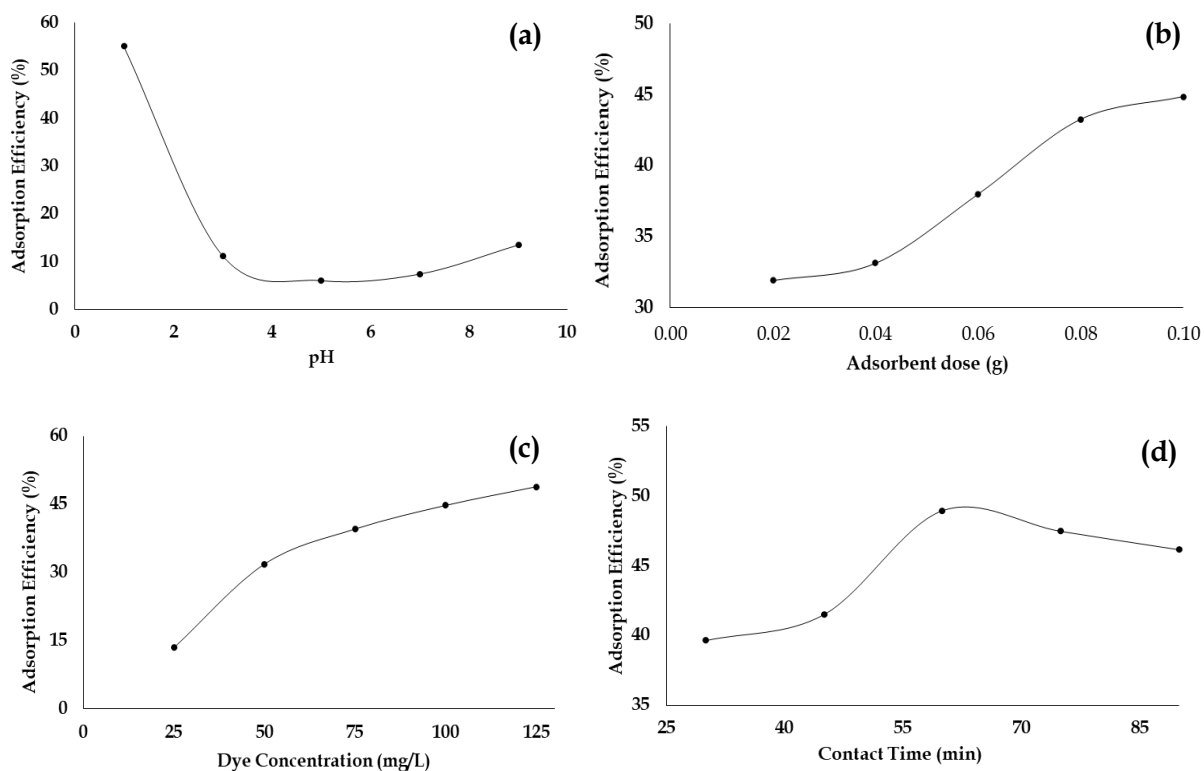


Figure 3. Effect of (a) pH, (b) adsorbent dose, (c) dye concentration, and (d) contact time on RBBR dye adsorption onto the activated carbon/alginate/chitosan composite beads

As seen in Figure 3(a), adsorption efficiency drops as solution pH rises. In this work, the ideal adsorption efficiency of composite beads made of activated carbon, alginate, and chitosan was at pH 1. At low pH levels, where the adsorbent surface is positively charged, there is a tendency for the adsorption of dye molecules to increase due to the electrostatic attraction between the adsorbent surface and the anionic dye molecules [14]. Chitosan becomes protonated at low pH levels due to the presence of H^+ , with the dominating form being $-NH_3^+$. In this instance, the anionic dye compound RBBR interacts electrostatically with the adsorbent with ease, increasing the dye removal value. The adsorbent is better suited for adsorbing dyes, resulting in this occurrence. This was in line with a previous study [32]. Meanwhile, at high pH levels, the adsorbent surface has a negative charge due to the deprotonation of active sites

like OH becoming O⁻, which aids in the reduction of dye adsorption due to electrostatic repulsion between anionic dye molecules and the adsorbent surface. In addition, the presence of OH⁻ will make RBBR compete to interact ionically with the adsorbent. Thus, the dye removal value will not be higher than in acidic conditions [3].

The adsorption efficiency versus the adsorbent dosage is shown in Figure 3(b). As the dosage of adsorbent was raised, caused the percentage of adsorption also rose. Increasing active sites on the adsorbent's surface is caused by increased adsorbent dosage. Therefore, more dye molecules can adsorb to the adsorbent's surface. However, a higher dosage of the adsorbent resulted in the adsorbent aggregating, which decreased the surface area and, ultimately, the adsorption efficiency decreased. In this investigation, the ideal dosage of composite bead for RBBR adsorption was 0.08 g, and it had an adsorption rate of more than 80% for RBBR dye. The optimum adsorbent dose in this study was much less than in the previous study [32], namely 2 g, with an adsorption efficiency of 80%.

According to Figure 3(c), the RBBR dye solution at 125 mg/L concentration produced an adsorption efficiency of about 48.9%. The adsorbent's adsorption rate decreases with decreasing RBBR dye solution concentration. The saturation of the adsorbent of activated carbon/alginate/chitosan composite beads against the adsorbate of dye molecules in the solution is not visible. According to the molecular collision concept, more molecules hit and react with the adsorbent as the concentration of RBBR dye increases, enhancing adsorption efficiency. This result is similar to the previous study [32].

The impact of contact duration on the activated carbon/alginate/chitosan composite beads' ability to adsorb dyes is depicted in Figure 3(d). Because the adsorbent's active sites are still empty at the start of the contact time, the dye molecules can readily cling to the surface of the adsorbent, leading to high adsorption efficiency. When the contact time was increased, the adsorbent's adsorption capacity for the RBBR dye grew progressively; however, after 60 min, the adsorption efficiency for the RBBR dye dropped. The saturation in the active sites on the adsorbent is the cause of the decline in adsorption efficiency. The optimum contact time of this study was shorter than that of previous studies on the adsorption of RBBR dye using activated carbon from *Thuja orientalis* leaves [32].

Kinetic Study of Adsorption

A kinetic study of RBBR dye adsorption using a pseudo-first-order reaction model, a pseudo-second-order, and an intraparticle diffusion model is shown in Figure 4a-c. A summary of the parameter calculations for each model is shown in Table 1.

The adsorption reaction of RBBR dye using composite adsorbent follows a pseudo-second-order response due to the highest correlation coefficient, $R = 0.9908$, compared to other models. This indicates that chemisorption is possibly the rate-limiting step that controls the adsorption process, in addition to different mechanisms, such as the electrostatic attraction of anionic RBBR dye with active sites on the composite surface [20]., in line with the FTIR data.

Table 1. Constants and correlation coefficients in the kinetic model of RBBR adsorption on composites

Parameter	Kinetics Model		
	Pseudo-first order	Pseudo-second order	Diffusion intraparticle
R ²	0.2936	0.9817	0.6211
q _e (mg g ⁻¹)	0.9789	1.8605	C=1.0584
Reaction rate constant (k)	k ₁ =0.0009 min ⁻¹	k ₂ =0.0620 g mg ⁻¹ min ⁻¹	k _{int} =0.0711 mg g ⁻¹ min ^{-1/2}

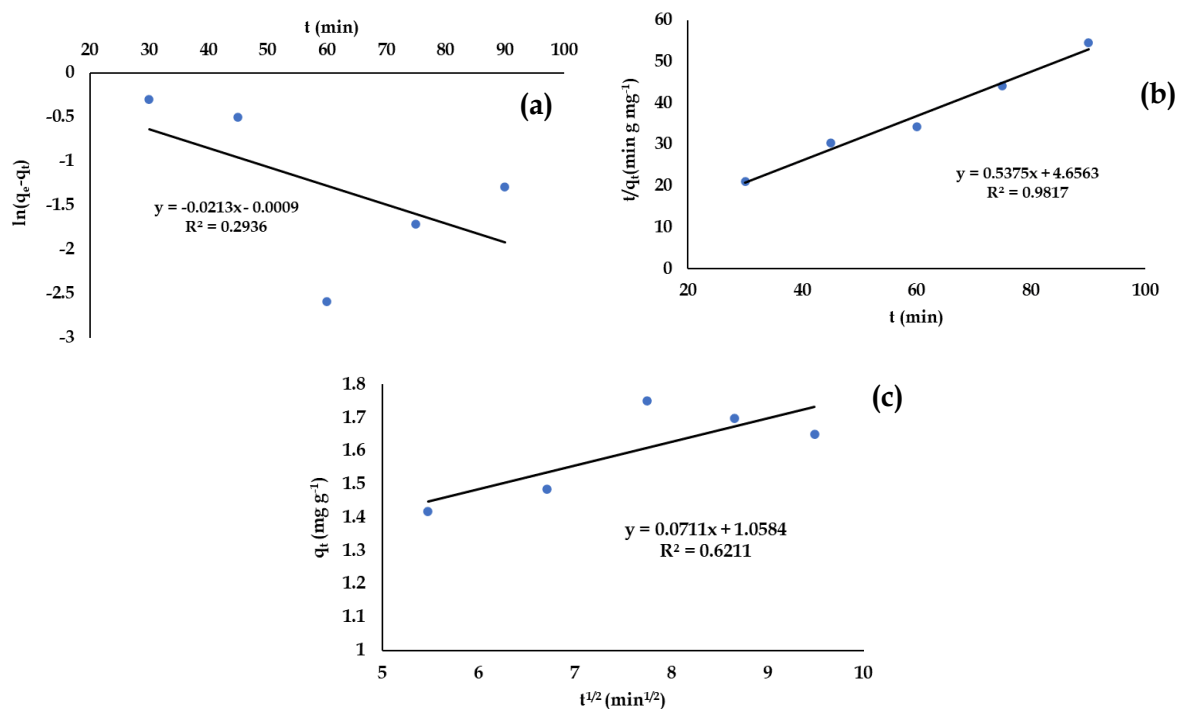


Figure 4. RBBR adsorption models: (a) pseudo-first-order reaction, (b) pseudo-second-order reaction, and (c) intraparticle diffusion model.

Isotherm Model for the Adsorption

The mechanism formed, and the process was described using the adsorption isotherm. When the adsorption process achieves an equilibrium state, the adsorption isotherm displays the state of the adsorption molecules dispersed between the liquid and solid phases. Adsorption isotherm analysis pertains to the widely recognized model of two isotherms (Langmuir and Freundlich) conducted at varying temperatures. Testing the linear regression equation of the Freundlich and Langmuir adsorption isotherms will reveal the kind of adsorption. The Langmuir isotherm was obtained using equations 1 and 2, and the curve was obtained by graphing C_e (ppm) and C_e/Q_e (Figure 4(a)). The Freundlich isotherm was obtained using equations 3 and 4 by plotting log Q_e vs. log C_e, as shown in Figure 4(b).

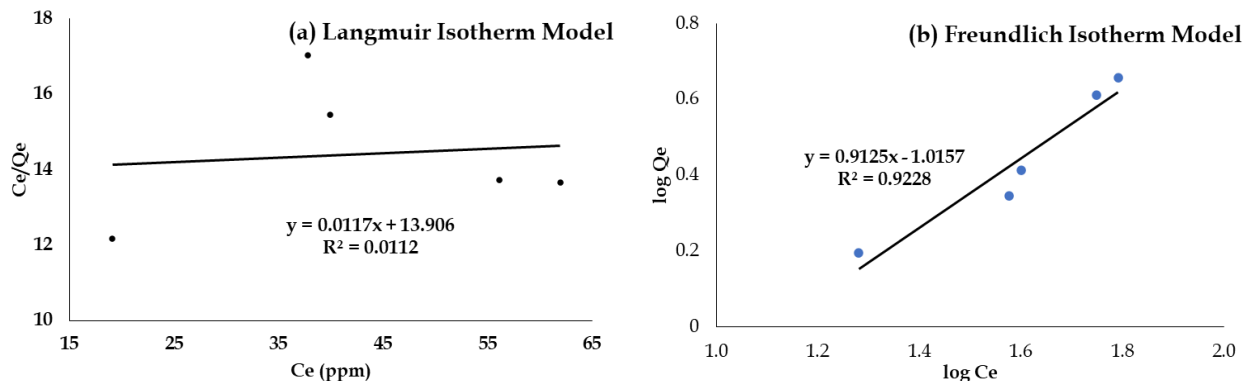


Figure 4. Isotherm model for the adsorption of RBBR dye solution

Langmuir's adsorption isotherm model is helpful for monolayer adsorption and supports adsorption on homogeneous adsorbent surface sites. At the same time, the isotherm model of Freundlich supports adsorption on surface heterogeneity and sites with different adsorption energy levels. The correlation coefficient, R^2 , compares how the isotherm equation is applied. According to Figure 4(a), the Langmuir isotherm model shows a coefficient of linearity (R^2) of 0.0112, whereas the graph of the Freundlich model in Figure 4(b) reveals a degree value (R^2) of 0.9228. An overview of the two isotherm models' computation calculations is shown in Table 2.

Table 2. RBBR dye's summary of Freundlich and Langmuir isotherm parameters

Model Isotherm	Regression	R^2	Q_m	K_L	K_f	n
Langmuir	$y = 0.0117x + 13.906$	0.0112	85.470	13.906	-	-
Freundlich	$y = 0.9125x - 1.0157$	0.9228	-	-	10.368	1.095

The linearity degree value (R^2) approaches the value of 1 to determine the equilibrium model. As a result, the adsorption isotherm utilized in this work is expected to follow the isotherm of Freundlich, which is consistent with earlier findings [8,14,35]. It was supported by FTIR data that several active sites of the composite play a role in adsorption (heterogeneous active sites), resulting in multilayer adsorption. The value of K_f and n in Freundlich's model indicates that the adsorbent and adsorbate have reached equilibrium. A positive charge value indicates an equilibrium, but a negative value means no equilibrium. The adsorption intensity value (n) is 1.095, and K_f is obtained as 10.368 L/g. There is an equilibrium because the result is positive. Therefore, activated carbon/alginate/chitosan composite beads are an effective adsorbent for removing RBBR dye. They have the potential to overcome the problem of water pollution by the dyes produced, one of which is from the textile industry. To be more economically profitable, efforts are needed to improve adsorption efficiency by modifying the composite structure, such as a layer-by-layer design.

Reusability Test

Since the second reuse, the composite has shown a decline in adsorption effectiveness. However, this decrease still suggests that the composite is suitable for reuse as an absorbent. Figure 5 demonstrates that the most significant reduction in reuse efficiency occurred in the

fifth cycle, with the remaining efficiency at 51.6%. Reusing the composite as an effective adsorbent is recommended until the fourth cycle (with adsorption effectiveness more significant than 60%). The use of NaOH performs well as a desorption agent, breaking the dye's RBBR bond with the composite, but also reduces adsorption effectiveness in the following cycle due to changes in the composite structure. The desorption process with dilute NaOH may affect the composite's active sites, specifically the deprotonation of amines, hydroxyls, and carbonyls. The %efficiency decrease was in line with previous research that utilized chitosan-alginate composite added with activated carbon from leather waste [36]. Similar research using activated carbon as an RBBR adsorbent also showed a decrease in efficiency of up to 73% in the fourth reuse [32].

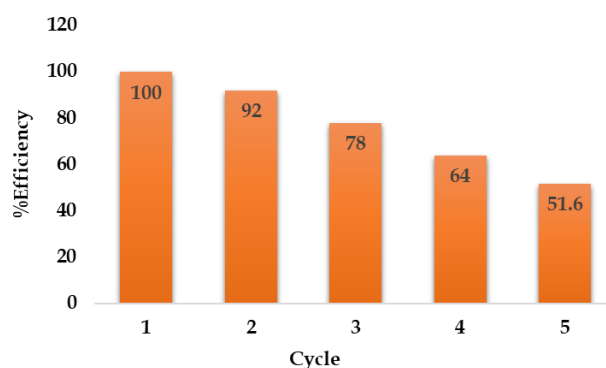


Figure 5. The %reuse efficiency adsorption in the composite life cycle.

Conclusion

A round activated carbon/alginate/chitosan composite bead with the properties of a solid, hard, black granular material with uniform size and shape was effectively synthesized. The composite has more protrusions, grooves, and asymmetric pores than activated carbon. FTIR analysis confirmed the enrichment of functional groups in activated carbon/alginate/chitosan composite, including OH, N-H, protonated amine, and carboxylate from the constituent polymers. These groups also serve as active sites for adsorbents. The composite's dye adsorption is most effective at pH 1, with an adsorbent dose of 0.08 g, a solution concentration of 125 mg/L RBBR dye, and a contact period of 60 minutes. The kinetic model of pseudo-second adsorption order indicates that chemisorption occurs in RBBR adsorption. The Freundlich isotherm model is suitable for composite beads, indicating heterogeneous or several active sites contributing to adsorption and resulting in multilayer adsorption. The synergistic characteristics of components play a crucial role in improving dye removal efficiency as well as the composite's endurance to acid and basic environments, proven by the effectiveness of reuse up to 4 times. Thus, based on sustainable natural resources, the activated carbon/alginate/chitosan composite beads offer a novel pathway for efficient color removal.

Acknowledgment

This research was funded by DIPA BLU Universitas Mataram through the University of Mataram's capacity improvement research scheme with contract number

1441/UN18.L1/PP/2024. We are grateful to the University of Mataram's Laboratory of Analytical Chemistry head and staff for providing all the equipment needed for this study.

References

- [1] H. Ben Slama *et al.*, "Diversity of synthetic dyes from textile industries, discharge impacts, and treatment methods," *Appl. Sci.*, vol. 11, no. 14, pp. 1-21, 2021, doi: 10.3390/app11146255.
- [2] S. Begum *et al.*, "Remarkable photocatalytic degradation of Remazol Brilliant Blue R dye using bio-photocatalyst 'nano-hydroxyapatite,'" *Mater. Res. Express*, vol. 7, no. 2, p. 25013, 2020, doi: 10.1088/2053-1591/ab6f3b.
- [3] O. A. Saputra, A. H. Rachma, and D. S. Handayani, "Adsorption of remazol brilliant blue R using amino-functionalized organosilane in aqueous solution," *Indones. J. Chem.*, vol. 17, no. 3, pp. 343-350, 2017, doi: 10.22146/ijc.25097.
- [4] G. A. L. Vieira *et al.*, "Marine associated microbial consortium applied to RBRR textile dye detoxification and decolorization: Combined approach and metatranscriptomic analysis," *Chemosphere*, vol. 267, 2021, doi: 10.1016/j.chemosphere.2020.129190.
- [5] E. Değerli, S. Yangın, and D. Cansaran-Duman, "Determination of the effect of RBRR on laccase activity and gene expression level of fungi in lichen structure," *3 Biotech*, vol. 9, no. 8, pp. 1-11, 2019, doi: 10.1007/s13205-019-1832-3.
- [6] L. D. Ardila-Leal, R. A. Poutou-Piñales, A. M. Pedroza-Rodríguez, and B. E. Quevedo-Hidalgo, "A brief history of colour, the environmental impact of synthetic dyes and removal by using laccases," *Molecules*, vol. 26, no. 13, 2021, doi: 10.3390/molecules26133813.
- [7] V. Parimelazhagan, P. Yashwath, D. Arukkani Pushparajan, and J. Carpenter, "Rapid Removal of Toxic Remazol Brilliant Blue-R Dye from Aqueous Solutions Using *Juglans nigra* Shell Biomass Activated Carbon as Potential Adsorbent: Optimization, Isotherm, Kinetic, and Thermodynamic Investigation," *Int. J. Mol. Sci.*, vol. 23, no. 20, pp. 1-33, 2022, doi: 10.3390/ijms232012484.
- [8] Z. Isik, M. Saleh, Z. Bilici, and N. Dizge, "Remazol Brilliant Blue R (RBRR) dye and phosphate adsorption by calcium alginate beads modified with polyethyleneimine," *Water Environ. Res.*, vol. 93, no. 11, pp. 2780-2794, 2021, doi: 10.1002/wer.1635.
- [9] J. Saleem, U. Bin Shahid, M. Hijab, H. Mackey, and G. McKay, "Production and applications of activated carbons as adsorbents from olive stones," *Biomass Convers. Biorefinery*, vol. 9, no. 4, pp. 775-802, 2019, doi: 10.1007/s13399-019-00473-7.
- [10] R. Ganjoo, S. Sharma, A. Kumar, and M. M. A. Daouda, "Activated Carbon: Fundamentals, Classification, and Properties," *Act. Carbon*, no. May, pp. 1-22, 2023, doi: 10.1039/bk9781839169861-00001.
- [11] M. A. Ahmad, M. A. Eusoff, P. O. Oladoye, K. A. Adegoke, and O. S. Bello, "Statistical optimization of Remazol Brilliant Blue R dye adsorption onto activated carbon prepared from pomegranate fruit peel," *Chem. Data Collect.*, vol. 28, p. 100426, 2020, doi: 10.1016/j.cdc.2020.100426.
- [12] E. Sanmuga Priya and P. Senthamil Selvan, "Water hyacinth (*Eichhornia crassipes*) - An

- efficient and economic adsorbent for textile effluent treatment – A review,” *Arab. J. Chem.*, vol. 10, pp. S3548–S3558, 2017, doi: 10.1016/j.arabjc.2014.03.002.
- [13] K. J. Lee, J. Miyawaki, N. Shiratori, S. H. Yoon, and J. Jang, “Toward an effective adsorbent for polar pollutants: Formaldehyde adsorption by activated carbon,” *J. Hazard. Mater.*, vol. 260, pp. 82–88, 2013, doi: 10.1016/j.jhazmat.2013.04.049.
- [14] N. L. Rahmah, N. Ismillayli, M. G. Darmayanti, and D. Hermanto, “Synthesis Activated Carbon / Chitosan / Pectin Composite as,” *AIP Conf. Proc.*, vol. 2720, no. 040005, pp. 1–7, 2023, doi: 10.1063/5.0136932.
- [15] M. A. K. Purnaningtyas, S. Sudiono, and D. Siswanta, “Synthesis of activated carbon/chitosan/alginate beads powder as an adsorbent for methylene blue and methyl violet 2b dyes,” *Indones. J. Chem.*, vol. 20, no. 5, pp. 1119–1130, 2020, doi: 10.22146/ijc.49026.
- [16] N. Ismillayli *et al.*, “Synthesize of self-electrostatic interaction chitosan-carrageenan membrane and its properties,” *J. Phys. Conf. Ser.*, vol. 1943, no. 012177, pp. 1–6, 2021, doi: 10.1088/1742-6596/1943/1/012177.
- [17] N. Ismillayli, H. Julianti, S. S. Handayani, and D. Hermanto, “Effect of Alginate-Chitosan edible film coating on vitamin c loss of fresh cut sliced pineapple (*Ananas comosus* (L.) merr),” *AIP Conf. Proc.*, vol. 2720, no. 040023, pp. 1–5, 2023, doi: 10.1063/5.0136933.
- [18] Y. Gao, Q. Yue, S. Xu, and B. Gao, “Activated carbons with well-developed mesoporosity prepared by activation with different alkali salts,” *Mater. Lett.*, vol. 146, pp. 34–36, 2015, doi: 10.1016/j.matlet.2015.01.161.
- [19] D. Hermanto, M. Mudasir, D. Siswanta, B. Kuswandi, and N. Ismillayli, “Optical fiber mercury biosensor based on immobilized urease and bromothymol blue onto the alginate-chitosan membrane in the flow-system,” *Kuwait J. Sci.*, vol. 49, no. 1, pp. 1–13, 2022, doi: 10.48129/kjs.v49i1.9400.
- [20] N. F. Al-Harby, E. F. Albahly, and N. A. Mohamed, “Kinetics, isotherm and thermodynamic studies for efficient adsorption of congo red dye from aqueous solution onto novel cyanoguanidine-modified chitosan adsorbent. *Polym.*, vol. 13, no. 4446, pp. 1–32, 2021, doi: 10.3390/polym13244446.
- [21] G. Hyldig, & Ditte, and M. B. Green-Petersen, “Quality Index Method-An Objective Tool for Determination of Sensory Quality,” *J. Aquat. Food Prod. Technol.*, vol. 13, no. 4, pp. 71–80, 2008, doi: 10.1300/J030v13n04.
- [22] T. K. Enock, C. K. King’ondy, A. Pogrebnoi, and Y. A. C. Jande, “Status of Biomass Derived Carbon Materials for Supercapacitor Application,” *Int. J. Electrochem.*, vol. 2017, pp. 1–14, 2017, doi: 10.1155/2017/6453420.
- [23] D. Hermanto, N. Ismillayli, R. Honiar, I. G. Ayu Sri Andayani, B. Mariana, and R. Kris Sanjaya, “Transparent Membrane of Polyelectrolyte Complex Doped with 2,6-Dichlorophenol-Indophenol as an Optical Sensor for Colorimetric Measurements of Ascorbic acid,” *Orient. J. Chem.*, vol. 36, no. 04, pp. 680–686, 2020, doi: 10.13005/ojc/360412.
- [24] A. A. A. Yaqin, S. Suherman, M. Mudasir, and D. Siswanta, “Carbon/Alginate/Chitosan Composite as a Sorbent for Solid-Phase Extraction and Preconcentration of Cu(II),”

Indones. J. Chem., vol. 22, no. 6, pp. 1469–1479, 2022, doi: 10.22146/ijc.70587.

- [25] A. Allwar, "Preparation and characteristics of activated carbon from oil palm shell for removal of iron and copper from patchouli oil," *Int. J. Appl. Chem.*, vol. 12, no. 3, pp. 183–192, 2016.
- [26] M. F. Queiroz, K. R. T. Melo, D. A. Sabry, G. L. Sasaki, and H. A. O. Rocha, "Does the use of chitosan contribute to oxalate kidney stone formation?," *Mar. Drugs*, vol. 13, no. 1, pp. 141–158, 2015, doi: 10.3390/md13010141.
- [27] A. B. D. Nandiyanto, R. Oktiani, and R. Ragadhita, "How to read and interpret ftir spectroscopy of organic material," *Indones. J. Sci. Technol.*, vol. 4, no. 1, pp. 97–118, 2019, doi: 10.17509/ijost.v4i1.15806.
- [28] Z. Belattmania *et al.*, "Isolation and FTIR-ATR and ¹H NMR characterization of alginates from the main alginophyte species of the atlantic coast of Morocco," *Molecules*, vol. 25, no. 18, pp. 1–9, 2020, doi: 10.3390/molecules25184335.
- [29] S. R. Dalal, M. H. Hussein, N. E. A. El-Naggar, S. I. Mostafa, and S. A. Shaaban-Dessuuki, "Characterization of alginate extracted from *Sargassum latifolium* and its use in *Chlorella vulgaris* growth promotion and riboflavin drug delivery," *Sci. Rep.*, vol. 11, no. 1, pp. 1–17, 2021, doi: 10.1038/s41598-021-96202-0.
- [30] V. B. V. Maciel, C. M. P. Yoshida, and T. T. Franco, "Chitosan/pectin polyelectrolyte complex as a pH indicator," *Carbohydr. Polym.*, vol. 132, pp. 537–545, 2015, doi: 10.1016/j.carbpol.2015.06.047.
- [31] A. Syafiuddin and M. A. Fulazzaky, "Decolorization kinetics and mass transfer mechanisms of Remazol Brilliant Blue R dye mediated by different fungi," *Biotechnol. Reports*, vol. 29, no. 00573, pp. 1–14, 2021, doi: 10.1016/j.btre.2020.e00573.
- [32] M. C. Arya, P. S. Bafila, D. Mishra, K. Negi, R. Kumar, and A. Bughani, "Adsorptive removal of Remazol Brilliant Blue R dye from its aqueous solution by activated charcoal of *Thuja orientalis* leaves: an eco-friendly approach," *SN Appl. Sci.*, vol. 2, no. 2, 2020, doi: 10.1007/s42452-020-2063-2.
- [33] A. Nasrullah, A. H. Bhat, A. Naeem, M. H. Isa, and M. Danish, "High surface area mesoporous activated carbon-alginate beads for efficient removal of methylene blue," *Int. J. Biol. Macromol.*, vol. 107, pp. 1792–1799, 2018, doi: 10.1016/j.ijbiomac.2017.10.045.
- [34] A. H. Jawad and A. S. Abdulhameed, "Facile synthesis of crosslinked chitosan-tripolyphosphate/kaolin clay composite for decolorization and COD reduction of remazol brilliant blue R dye: Optimization by using response surface methodology," *Colloids Surfaces A Physicochem. Eng. Asp.*, vol. 605, no. 125329, pp. 1–11, 2020, doi: 10.1016/j.colsurfa.2020.125329.
- [35] M. Saleh, M. Yalvaç, and H. Arslan, "Optimization of remazol brilliant blue r adsorption onto *xanthium italicum* using the response surface method," *Karbala Int. J. Mod. Sci.*, vol. 5, no. 1, 2019, doi: 10.33640/2405-609X.1017.
- [36] F. Melara *et al.*, "Synergistic effect of the activated carbon addition from leather wastes in chitosan/alginate-based composites," *Environ. Sci. Pollut. Res.*, vol. 28, no. 35, pp. 48666–48680, 2021, doi: 10.1007/s11356-021-14150-8.